NANOPARTICLE-BASED O_2 THERAPY ENHANCES TISSUE OXYGENATION AND REDUCES SECONDARY INJURY AFTER CERVICAL SPINAL CORD INJURY IN RATS

Jiamei Hou[1,2], Caleb Brown[2,1], Daniel Plant[1], Alexis Pullos[1], Kelena Klippel[2,1], Fiona Cheung[1], Shigeharu Tsuda[2,1], Araana Mondal[1], Cynthia S. Garvan[2], Bruce Spiess[2], Floyd J Thompson[1,3], Prodip Bose[1,2,4]

[1] North Florida/South Georgia Veterans Health System, Gainesville, FL; [2] Department of Anesthesiology, [3] Neuroscience, [4] Neurology, University of Florida College of Medicine, Gainesville, FL

INTRODUCTION

Cervical spinal cord injury (CSCI) is a devastating condition that results in permanent neurological deficits and remains a major cause of disability among Civilians, Service Members, and Veterans. While the initial mechanical trauma causes immediate damage to the spinal cord, secondary injury processes—including ischemia, hypoxia, oxidative stress, excitotoxicity, and neuroinflammation—continue to evolve over hours to days, leading to additional neuronal and axonal loss and worsening neurological outcomes. Targeting these secondary injury cascades represents a critical therapeutic opportunity; however, there are currently no clinically effective neuroprotective therapies that substantially improve recovery following acute CSCI. $NanO_2$ (NuvOx Therapeutics, Tucson, AZ) is a patented intravenous perfluorocarbon nanoparticle emulsion designed to enhance oxygen delivery to ischemic tissues and improve tissue oxygenation during the acute phase of injury. In this study, we evaluated the therapeutic efficacy of $NanO_2$ following experimental CSCI and tested the hypothesis that early treatment would reduce secondary injury, improve locomotor recovery, and promote neuroprotection.

MATERIALS AND METHODS

Adult (3 months old) female Sprague-Dawley rats (Charles River Laboratories, USA), weighing 250-300 g, were randomly assigned to the CSCI-$NanO_2$ and CSCI-Sal control groups. The contusion injuries were produced using the Infinite Horizons impactor device (Precision Scientific Instrumentation, Lexington, KY). A 2.5-mm impactor tip was set 5 mm above the spinal cord, and a contusion injury was created, with a force of 200 kilodynes (no dwell time) on the $C_{6/7}$ segment of the exposed spinal cord produced by laminectomy under general anesthesia and sterile conditions.

Drug and Drug Administration: Randomized $NanO_2$ (0.6 ml/kg) or NS was administered via the lateral tail vein 20 minutes after SCI, and 90 minutes apart three times in total. Animals were kept in an incubator in room air during the therapy and recovery.

The velocity-dependent ankle torque was tested in awake animals across a wide range of velocities (612 – 49 deg/sec) to permit analyses of tonic (low velocity) and dynamic (high velocity) contributions to lower limb spasticity using our previously published protocol (Bose et al., 2002; 2012 & 2013; Thompson et al., 1996; Hou et al., 2014 & 2020).

Tibial /plantar H-reflex rate depression was measured by stimulation of the tibial nerve using 200-µs pulses at 3-sec inter-stimulus intervals during a frequency series (0.3, 0.5, 1, 2, 3, 4, 5, 10, and 0.3 Hz) after a non-invasive procedure (Bose et al., 2012 & 2013; Thompson et al., 1992; 1993; 1998; 2001; Hou et al., 2020).

Gait/locomotion was evaluated with Simi Motion 2D/3D Systems (SIMI Reality Motion Systems GmbH, Germany) analysis and CatWalk XT footprints (Noldus Information Technology, Leesburg, VA) using our previous protocol (Hou et al, 2014; 2020).

MRI images were collected on a 7T Preclinical MRI system (MR Solutions Inc., UK). The MRI data were collected on a 7T/17 cm scanner from MR Solutions, Guilford, UK, using a quadrature rat body coil. The animals were anesthetized with 4% isoflurane in O_2 at a flow rate of 1 L/minute. The body temperature of the animal was maintained in a cradle using a warm air recirculation system operating at 37°C. Respiration was monitored (SA Instruments Inc., Stony Brook, NY) using a pillow sensor under the abdomen and maintained at approximately 40 beats per minute by adjusting the isoflurane levels between 1-2%. Motion in the thoracic area was carefully restricted using tape, and respiratory gating was not necessary. The sagittal T2-weighted Fast Spin-Echo images were collected with a matrix size of 512 x 512 and a field-of-view of 50 x 50 mm. Twelve contiguous 0.5 mm thick slices were collected centered on the spinal column. The initial TE was 36ms, and the echo train was 16 with an interval of 12ms. Two averages were collected, resulting in a total experimental time of 11 minutes.

Immunohistochemistry: Animals were perfused with 4% paraformaldehyde in phosphate buffer. The spinal cord tissue was collected and sectioned coronally at a thickness of 40 µm and incubated with primary antibodies against NeuN (1:1,000), 3-NT (1:200), and IL-1β (1:250), along with appropriate secondary antibodies. The staining was qualitatively analyzed, and pictures were taken with a Zeiss confocal microscope (LSM 710, Carl Zeiss, Oberkochen, Germany) for further analysis.

RESULTS

Fig. 1.

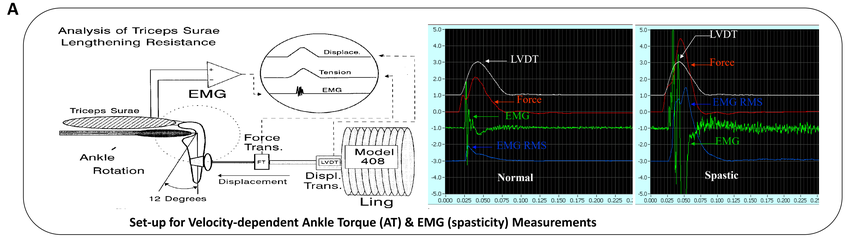

Fig.1. A. Instrumental Set-up and Example Waveforms for Velocity-dependent Ankle Torque & EMG (spasticity) Measurements. **B.** Velocity-dependent ankle torque measurements showed that $NanO_2$-treated CSCI animals exhibited a marked reduction in spasticity compared to saline-treated CSCI controls. **C.** The time-locked EMGs showed a similar pattern. *, p<0.05, **, p<0.01, compared to normal animals; ^, p<0.05, compared to the same group at PO Mon 1; !, p<0.05, !!, p<0.01, !!!, p<0.001, compared to CSCI-$NanO_2$ at the same time points. One-way ANOVA.

Fig. 2.

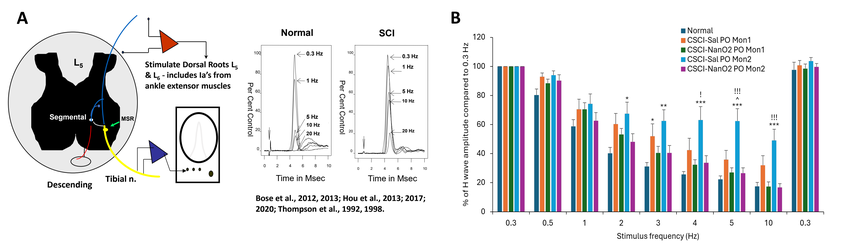

Bose et al., 2012, 2013; Hou et al., 2013; 2017; 2020; Thompson et al., 1992, 1998.

Fig.2. A. H-reflex and example Waveforms for H-reflex Rate Depression. **B.** $NanO_2$-treated CSCI animals revealed better normalization of H-reflex compared to saline-treated CSCI control animals. *, p<0.05; **, p<0.01; ***, p<0.001, compared to normal; ^, p<0.05, compared to the same group at PO Mon 1; !, p<0.05; !!!, p<0.001, compared to CSCI-$NanO_2$ at the same time points. One-way ANOVA.

Fig. 3.

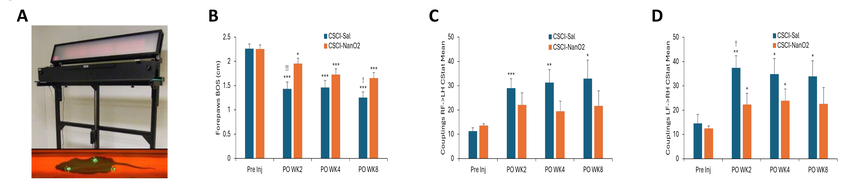

Fig.3. Catwalk footprint analysis (**A**) showed improved forepaw base of support (**B**), couplings of RF->LH (**C**), and LF->RH (**D**) in $NanO_2$-treated animals when compared to saline-treated CSCI control animals. *, p<0.05 ; **, p<0.01; ***, p<0.001, compared to Pre Inj; !, p<0.05, !!, p<0.01, compared to CSCI-$NanO_2$ at the same time points. One-way ANOVA.

ACKNOWLEDGEMENTS

This work was supported by Department of the Army – USAMRAA HT9425-23-1-0562 (SC220248). We thank Dr. Evan Unger, Executive Chairman and Co-Founder of NuVox Pharma, for providing $NanO_2$.

Fig. 4.

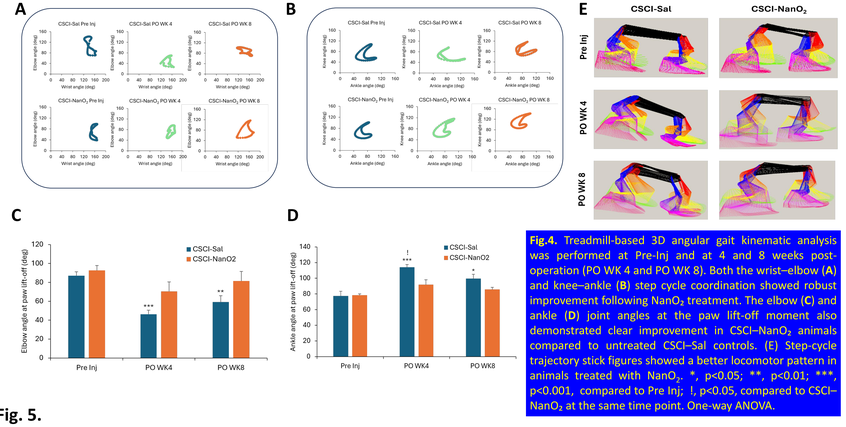

Fig.4. Treadmill-based 3D angular gait kinematic analysis was performed at Pre-Inj and at 4 and 8 weeks post-operation (PO WK 4 and PO WK 8). Both the wrist–elbow (**A**) and knee–ankle (**B**) step cycle coordination showed robust improvement following $NanO_2$ treatment. The elbow (**C**) and ankle (**D**) joint angles at the paw lift-off moment also demonstrated clear improvement in CSCI–$NanO_2$ animals compared to untreated CSCI–Sal controls. (**E**) Step-cycle trajectory stick figures showed a better locomotor pattern in animals treated with $NanO_2$. *, p<0.05; **, p<0.01; ***, p<0.001, compared to Pre Inj; !, p<0.05, compared to CSCI–$NanO_2$ at the same time point. One-way ANOVA.

Fig. 5.

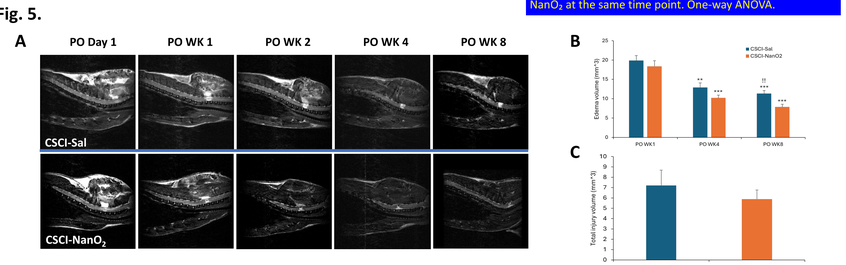

Fig.5. Sagittal T2-weighted fast spin-echo images were acquired at post-operative (PO) Day 1, and at PO Weeks 1, 2, 4, and 8. Representative time-series images from one CSCI–Sal and one CSCI–$NanO_2$ animal are shown in panel (**A**). The $NanO_2$-treated animal exhibited a smaller injury volume at all examined time points compared with the CSCI–Sal control. In vivo edema volume (**B**) and ex vivo total injury volume (**C**) were quantified using VivoQuant software. The data demonstrated a significant reduction in edema volume at PO Week 8 and a trend toward reduced total injury volume in CSCI–$NanO_2$ animals compared with CSCI–Sal controls. **, p<0.01, ***, p<0.001, compared to the same group at PO WK 1; !!, p<0.01, compared to CSCI-$NanO_2$ at the same time point. One-way ANOVA.

Fig. 6.

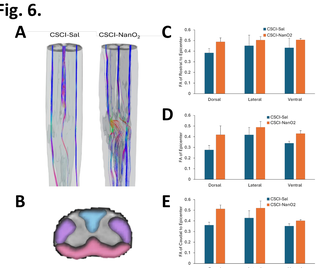

Fig.6. DTI tractography images showed more preserved descending motor fibers across the injury epicenter in the $NanO_2$-treated animal compared to the Sal-treated animal (**A**). The three regions of interest (dorsal, lateral, ventral) of the spinal cord used for FA analysis are shown in **B**. The FA of the rostral to epicenter (**C**), epicenter (**D**), and caudal to epicenter (**E**) showed the trends of improvement in all 3 ROIs in treated animals compared to Sal animals.

Fig. 7.

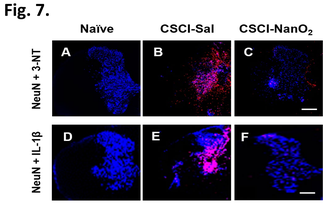

Fig.7. $NanO_2$-treated animal showed a significant decrease in oxidative stress markers 3-NT (**A-C**) and pro-inflammatory cytokines IL-1β (**D-F**) in spinal cord tissue, close to the injury epicenter. Scale bar: 200 µm.

CONCLUSIONS

1. The CSCI–Sal animals showed significant increases in ankle torque (AT) at both tested time points (**Fig. 1**) compared with naïve controls, indicating enhanced spasticity. In contrast, $NanO_2$-treated animals exhibited markedly reduced spasticity (**Fig. 1**).
2. The beneficial effects of $NanO_2$ treatment may be related to its ability to limit secondary injury processes and promote normalization of spinal segmental synaptic plasticity (**Fig. 2**). Specifically, recovery of inhibitory sensory afferent transmission to motoneurons (EPSPs), along with upregulation of GABA/$GABA_B$ and central descending noradrenergic (NA) systems, may help suppress the development of maladaptive neuroplasticity, such as increased persistent inward currents (PICs) typically observed at one month post-injury in SCI animals, that contribute to sustained spasticity. These therapy-induced modulations of spinal regulatory circuitry likely underlie the efficacy of $NanO_2$ treatment initiated at the acute injury phase.
3. Acute $NanO_2$ therapy also led to significant improvements in gait and paw movement parameters as assessed by CatWalk gait analysis (**Fig. 3**). Moreover, 3D angular kinematic analysis revealed superior recovery of gait coordination in $NanO_2$-treated animals compared with CSCI controls (**Fig. 4**).
4. MRI evaluations demonstrated reduced lesion cavity and edema volumes, as well as better preservation of spinal cord fibers, in $NanO_2$-treated animals relative to saline-treated CSCI animals (**Figs. 5–6**). Immunohistochemical analysis further revealed significantly lower expression of pro-inflammatory and oxidative stress markers in $NanO_2$-treated tissue compared with CSCI–Sal controls (**Fig. 7**).
5. Collectively, these behavioral, physiological, MRI, and histological findings indicate that $NanO_2$ therapy mitigates ischemia-mediated neurological damage and improves motor function following spinal cord injury. The observed neuroprotective and functional benefits suggest strong translational potential of $NanO_2$ therapy for human SCI.